Algerian Journal of Engineering and Technology

Journal homepage: https://jetjournal.org/index.php/ajet

Original Article

Contribution to characterization of the Zinc retention by marl collected from the aquifer substratum

Mourad Bellaloui*, Messaoud Bennemla, Farida Semaoune, Djamel Larbaoui, Djaber Otsmane, Yasmine Melhani, Amina Amrane, Samia Ladjouzi

Nuclear Research Center of Draria, Algiers, Algeria

ARTICLE INFO

Article history:
Received 05 October 2023
Revised 02 November 2023
Accepted 07 November 2023

Keywords:
Adsorption;
Zinc;
Marl;
Isotherm;
substratum.

ABSTRACT

Two samples (S20 and S6) of marl are collected from aquifer substratum of the watershed of Wadi El-Ghoula in order to make a comparative study to remove Zinc from solution. The DRX analysis indicate five phases Montmorillonite, Illite, Kaolinite, Calcite and Quartz X-Fluorescence shows the predominance of silica, alumina and lime. In FTIR analysis, all bands are identified for S20, S6. The specific surface area for S20 and S6 are equal respectively to 21.6206 m^2/g and 24.6445 m^2/g and our materials have a meso-porous character. The retention capacity at equilibrium for S20 and S6 are equal respectively to 9.94 (mg/g) and 9.87 (mg/g). Liquid film diffusion and intraparticle diffusion models control simultaneously the process of adsorption of zinc in Marl. Non-linear treatment gives Langmuir and Temkin as best model for S20 and Freundlich for S6. Radlish-Peterson is the best model for S20 but for S6 the best model is given simultaneously by Sips and Radlish-Peterson. The values of AIC and AICc give a good opportunity to separate between used isotherms models.

1. Introduction

Heavy metals are present in the air, soil and water. They are also present in flora, fauna and in our bodies. These heavy metals are at minimal levels. The important industrialization in the world has increased their concentration in the environment by anthropic contamination.

The health risk caused by the presence of heavy metals in water is known and several researches have been made to identify their effects. The objective of all treatment techniques is to eliminate contamination or reduce it to acceptable levels at the lowest possible cost.

There are two types of treatment for toxic heavy metals: conventional and non-conventional treatments. Conventional treatment methods are characterized by high consumption of energy and chemical compounds and the production of large amounts of waste. Non-conventional treatments are characterized by low consumption of chemical compounds, energy, and produce small amounts of waste.

The old conventional treatment is the all-chemical processes that includes precipitation complexation and solvent extraction [1-2]. The electrochemically technics, another conventional method, based on cathode electrodepositing or associated with separate methods like electrodialysis, osmosis or reverse osmosis [1-2].

The adsorption technic by synthetic or natural materials is a good opportunity. For the synthetic material, Zeolite and resin are the typically example to use [5-7]. An example of naturel material is the biosorbent, an organic compound having a possibility to adsorb heavy metals [3]. Another example is the use of clay material or bentonite to remove toxic heavy metals [4].

Our study concerns the use of two samples of marl taken from the bedrock of the Wadi Al-Ghoula aquifer, which is located near the city of Draria. It is planned to use this material as an adsorbent of the toxic heavy metal Zinc. The two samples studied were taken by drilling core samples. The first sample, named S20, was taken far from the bed of

* *Corresponding author*. Tel.: +213 5 52 26 80 95
E-mail address: m-bellaloui@crnd.dz

Peer review under responsibility of University of El Oued.

 https://dx.doi.org/10.57056/ajet.v8i2.124

the Wadi Al-Ghoula at a depth of twenty meters. The second sample, named S6, was taken near the bed of the Wadi Al-Ghoula at a depth of six meters.

These two marl samples will be used to remove Zinc from a synthetic aqueous solution. As a reminder, the limit values of Algerian standards and the World Health Organization (WHO) limit value for the concentration of Zinc in drinking water is equal to 5 mg/L [8][9].

Zinc, like other metals, is essential to metabolism, plays a role in cellular metabolism and the immune system at low doses [11]. However, at higher concentrations it becomes toxic to the body.

Zinc is found in various industrial processes, for example in electroplating, alloy metallurgy, pigments and paints, pesticides and chemical synthesis [8][10].

The first objective of our work is the characterization study of two samples of marl (S20, S6), this characterization concerns essentially the determination of the specific surface area (BET), the determination of the mineralogical phases by the technique of XRD, the functional analysis by FTIR and the characterization of the composition by X-ray fluorescence.

The second objective is the study of retention for the two samples (S20, S6) which will be done in batch with an optimization of the parameters of adsorption. A kinetic study will follow and our work will be finalized by a study of the isotherms by using models with two parameters and three parameters. The treatment of the results will be done in nonlinear mode

A comparative study on the results obtained for the two marl samples (S20, S6) in the characterization and in the retention study.

To differentiate the results, some classical coefficients will be used such as the coefficient of determination R2, its adjusted form R2adj and the nonlinear $\chi 2$ chi-square test. Other less known and less used coefficients which are the Akaike information criterion AIC and its corrected form AICc are used. This will allow us to compare them with the classical coefficients.

1.1. Geological consideration

The geology of the watershed of the Oued el Ghoula is made up of:

- A superficial layer which corresponds to the vegetable ground of a thickness which varies between 0.5m to 2m
- A sandy formation with very little clay and a clay-loam formation with intercalations of sandstone-limestone levels attributed to the Astian. Its thickness is 5m for the borehole corresponding to sample S6 and 24m for the borehole of sample S20.
- A Plaisancian layer formed by marly clays of blue-grey color fossiliferous at the top.

2. Materials and Methods

2.1. Material

To collect samples in the substratum of the aquifer of the watershed of Wadi El-Ghoula, two boreholes were executed, the first (named S20) at 20 meters depth and the second (named S6) at 6 meters depth.

The samples are dried at room temperature and sieved through an 80 micron sieve before being used. The fraction of samples smaller than 80 microns was homogenized and used in our work. 120mL HDPE bottles are used to shake the samples. A zinc solution is prepared with anhydrous zinc sulfate from Merck. All solutions are prepared with deionized water.

Nitric acid solution (0.1M) and sodium hydroxide solution (0.1M) are used to adjust the pH.

The adsorption coefficient at equilibrium qe (mg/g) and the retention percentage are retained for monitoring the retention process and its two parameters are defined by:

$$q_e = \frac{V}{m}\left(C_i - C_e\right) \qquad (1)$$

$$retention(\%) = \frac{C_i - C_e}{C_i} \qquad (2)$$

Where:

q_e: The adsorption coefficient at equilibrium (mg/g)
V: the volume of solution (L).
M: the weight of the adsorbent (g).
C_i: the initial concentrations (mg/L).
C_e: the concentration at equilibrium of adsorbent (mg/L).

The FTIR characterization analysis is done with a Perkin-Elmer equipment, the sample is placed directly in the measuring cell without any preparation.

After a determined time of agitation, the samples are centrifuged for 30 minutes at 3000 rpm. The supernatant is collected and the residual zinc is analyzed by a GBC atomic absorption spectrophotometer model Avanta Sigma.

The measurement of the specific surface area (BET) is obtained by adsorption using one gram of sample, previously dried at 200°C in an inert atmosphere of nitrogen, using a Micrometritics brand surface analyzer.

2.2. Fitting and error calculus

Excel from Microsoft Office gives a possibility to fit non-linear models to data by using Solver function.
The sum of the squared difference "(SSE)" (equation (3)) between data point (experimental results) and the function describing the data are minimized via an iterative algorithm by using Solver [12-14].

$$SSE = \sum_{i=1}^{n}\left(q_{e,calc} - q_{e,meas}\right)_i^2 \quad (3)$$

According to literature, the non-linear coefficient of determination R2 (equation (2)) and the adjusted coefficient of determination R2adj (equation (3)) are used to evaluate obtained results.

$$R^2 = 1 - \frac{\sum\left(y - \hat{y}\right)^2}{\sum\left(y - \bar{y}\right)^2} \quad (4)$$

$$R_{adj}^2 = 1 - \frac{(n-1)}{(n-p)} \times \left(1 - R^2\right) \quad (5)$$

y: dependent parameter.
$\bar{y}$: mean valus.
$\hat{y}$: fitted value.
n: samples number.
p: is number of parameters.
the Akaike Information Criterion AIC is given by equation (04) and equation (06)

$$AIC = 2p - 2\ln(L) \quad (6)$$

With

$$\ln(L) = 0.5 \times \left(-N \times \left(\ln(2\pi) + 1 - \ln N + \ln \sum_{i=1}^{n} \chi_i^2\right)\right) \quad (7)$$

And where

$\sum_{i}^{n} \chi_i^2$: the residual from the non linear square fit and

N : their number.

Another simplified form of this equation is:

$$AIC = 2p - n\left[\ln\left(\frac{SEE}{(n-p)}\right)\right] \quad (8)$$

To improve quality of AIC , a corrected form of this parameter AICc is giving by equation (9):

$$AICc = AIC + \frac{2p(p+1)}{n-p-1} \quad (9)$$

AIC allows to penalize models depending on the number of parameters. Model with the lowest value of AIC is best one. If the number of points is small, AICc is used.

The non-linear chi-square test χ^2 is used and its equation is defined by equation (10):

$$\chi^2 = \sum_{i=1}^{n} \frac{\left(q_{e,calc} - q_{e,meas}\right)^2}{q_{e,meas}} \quad (10)$$

$q_{e,meas}$: the experimental capacity of retention.
$q_{e,calc}$: the retention capacity of the model.

3. Result and Discussion

3.1. Samples characterization

The results obtained by XRF (Table 1) show the predominance of three compounds: silica, alumina and lime. They represent a weight percentage for S20 and S6 respectively equal to 66.17 % and 69.24 %. The Mass ratio SiO2/Al2O3 obtained for S20 and S6 are respectively equal to 3.25 and 2.91. These values are due to the high value of free silica. As these values are between 2 and 5.5, they are characteristic of montmorillonite
The FTIR spectrum gives the variation of transmi²ttance percentage as a function of wave number. The FTIR spectra (Fig. 1a and Fig. 1b, Table 2) of samples S20 and S6 show respectively two bands located at 3623.1 cm^{-1} and 3621.9 cm^{-1} corresponding to the OH stretching vibration of silanol groups.
The two bands located at 3392.2 cm^{-1} and 3390.8 cm^{-1} correspond to the OH stretching vibration of H2O for samples S20 and S6 respectively.
The band at 1003.8 cm^{-1} corresponds to the stretching vibration of Si-O-Si for S20 and for S6 the value is at 1002.1 cm^{-1}.
The bands observed at 878.5 cm^{-1} and 873.6 cm^{-1} correspond to the deformation vibrations of Al-OH-Al for S20 and S6 respectively.
The Si-OH band of quartz is located at 778.5 cm^{-1} and 778.9 cm^{-1} for S20 and S6 respectively [15].
The three bands at 797.8 cm^{-1}, 527.3 cm^{-1} and 463.1 cm^{-1}

correspond to the Si-O deformation vibration for S20. For S6, the three bands are at 798.1 cm^{-1}, 526.9 cm^{-1} and 466.8 cm^{-1}[16].

The three bands identifying calcite for S20 in the stretching vibrations are at 1424.5 cm-1, 873.0 cm^{-1} and 712.5 cm^{-1}. For S6, the three bands are at 1430.7 cm^{-1}, 873.5 cm-1 and 712.5 cm^{-1} [17].

The specific surface area according to BET results for S20 and S6 is equal to 21.62 m^2/g and 24.65 m^2/g respectively (Table 3). The micropore volume for S20 and S6 is equal to 0.001291 cm^3/g and 0.001371 cm^3/g respectively (Table 3). The average pore diameter is equal to 78.56 Å for S20 and 69.41 Å for S6 (Table 3). Thus, our materials present a meso-porous character The DRX analysis indicates that our marl samples S6 and S20 are composed qualitatively by five phases, which are Montmorillonite, Illite, Kaolinite, Calcite and Quartz (Fig. 2a and 2b).

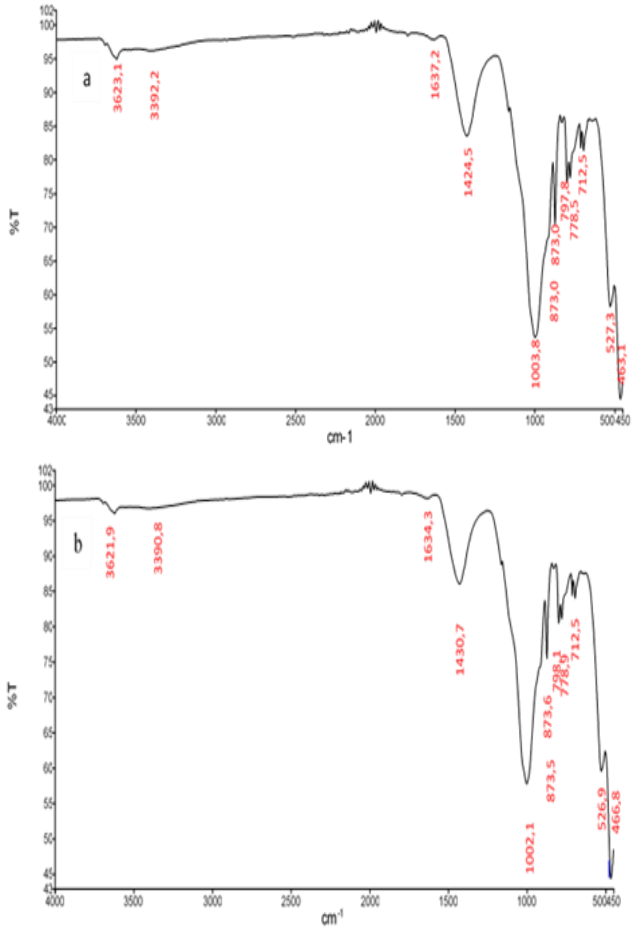

Fig 1. FTIR of samples ((a)- S20 and(b)- S6)

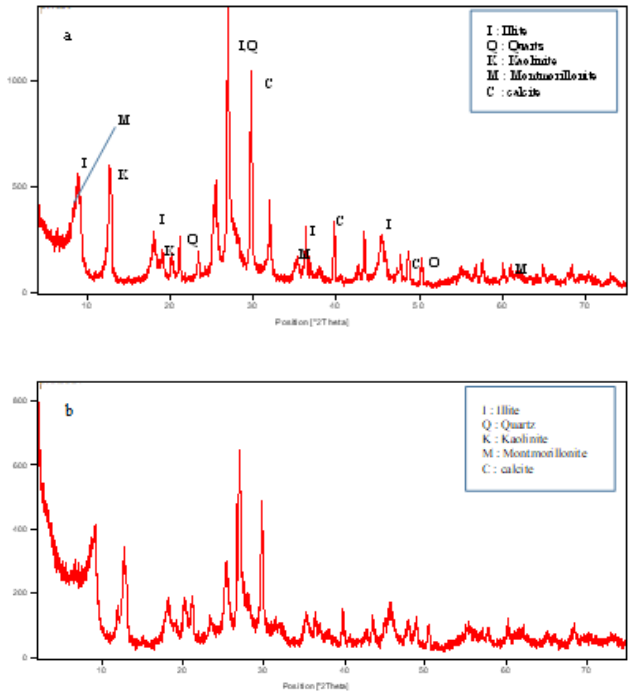

Fig 2. XRD of a-S20, b-S6

Table 1: Chemical composition of Marl

	Marl (wt %)										
	SiO_2	Al_2O_3	CaO	Fe_2O_3	MgO	Na_2O	K_2O	TiO_2	P_2O_5	SO_3	MnO
S20	39.2	12.05	14.92	4.51	1.76	0.84	1.70	0.56	0.21	0.23	---
S6	41.46	14.25	13.53	4.58	1.80	1.07	1.74	0.56	0.21	0.29	0.04

Table 2: BET characterization of S20 and S6

	Micro pores volume (cm^3/g)	Specific surface area BET (m^2/g)	Average pore diameter (Å)
S20	0.001291	21.62	78.56
S6	0.001371	24.65	69.41

3.2. Adsorption Study

3.2.1. Parameters optimization of adsorption

The pH optimization for both samples S20 and S6 gives: From pH=2 to pH=7, the retention capacity qe of Zinc increases. At 2≤ pH ≤4, there is adsorption competition between H+ and Zn^{2+}. When pH ≥4, the hydronium ion concentration decreases and the retention of $Zn^{2+}$by the adsorbent increases and a plateau is obtained. At pH ≥7.3 $Zn(OH)_2$ begins to form respectively (Fig. 3.) [15] [18,19]. The pH=5.5 ± 0.2 is chosen as the working pH for the two samples.

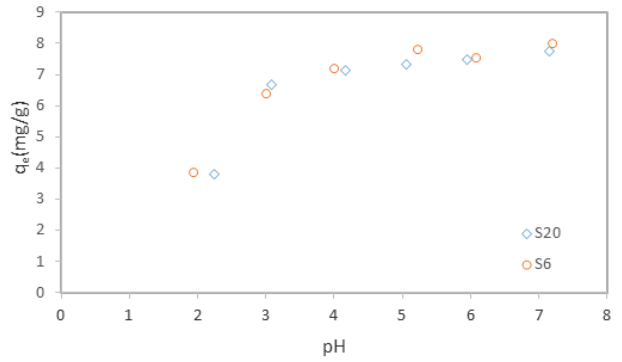

Fig 3. Optimization of Zinc pH adsorption by marl. The operatory conditions are: Vs= 0,04L, Ci= 20 mg/L and shaking period = 60 min at 150rpm.

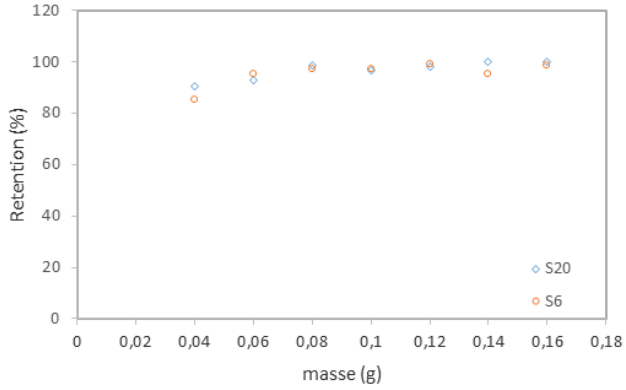

Fig 4. Optimization of Zinc mass adsorption by marl. The operatory conditions are : Vs=0,04L,Ci= 20 mg/L, , pH=5,5±0,2 and shaking period =60 min at 150rpm

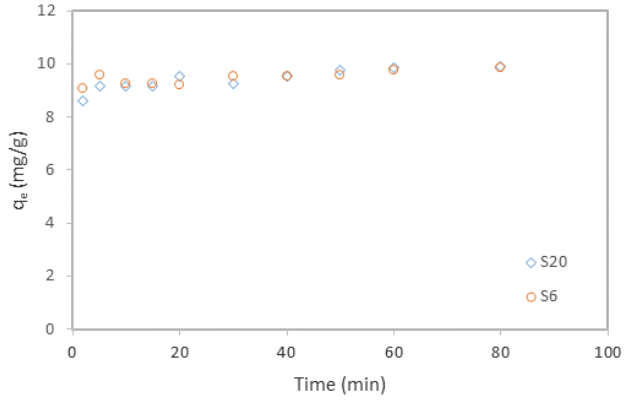

Fig 5. Optimization of Zinc mass adsorption by marl. The operatory conditions are : Vs= 0,04L, Ci=20 mg/L, pH =5,5 ± 0,2 and m=0.08 g.

3.2.2. Kinetic and diffusion models

The adsorption process takes place in three stages [20]: in the first, the adsorbate is transferred to the interface. In the second step, the adsorbate is diffused through the interface, this step is called film diffusion or external diffusion. In the third step, there is transfer in the particle, this transfer is managed by intra-particular diffusion or internal diffusion. Finally, we have the retention of the adsorbate in the active site.

The adsorption process was defined by the slowest step [21]. Diffusion in the film and/or intra-particular diffusion, corresponding respectively to the second and the third stage, which are the slowest stages of the process [20].

The pseudo-first order model or Lagergren model, based on the solid capacity [22], is expressed in linear form:

$$\log\left(q_e - q_t\right) = \log q_e - \frac{k_1}{2.0303}t \qquad (11)$$

k_1: speed constant (min^{-1}).

q_e: the retention capacity at equilibrium (mg/g).

q_t: the retention capacity at corresponding time (mg/g).

A plot of $\log(q_e - q_t) = f(t)$, gives k_1 and q_e from the slope and intercept respectively.

The pseudo-second order rate or Ho's second order rate equation and its linear form is given by equation (12) :

$$\frac{t}{q} = \frac{1}{q_e^2 k_2} + \frac{1}{q_e}t \qquad (12)$$

k_2 speed constant of pseudo-second order (g mmole/min).

The values of k_2 and qe are determined from slope and intercept of plots of t/q=f(t) [23].

To study the adsorption diffusion at the liquid-solid interface, the most used models in the literature are the liquid film diffusion and the intraparticle diffusion.

The liquid film diffusion model is defined by equation (13):

$$\ln(1-F) = -k_{fd}\,t \text{ [24]} \qquad (13)$$

$F = \frac{q_t}{q_e}$ the fraction of solute adsorbed.

k_{fd} the rate constant

The equation of intraparticle diffusion model was given by

$$q_t = k_i t^{1/2} + C_i \text{ [24]} \qquad (14)$$

Where

k_i: the diffusion rate constant.

C_i: the intercept.

The kinetic curves (Fig. 6.) show that the adsorption of Zn^{2+} in samples S20 and S6 follows the pseudo-second order model with a coefficient of determination equal to R^2=0.999.

Table 4 shows the results of the comparison of the retention of our marl samples and with other adsorbents. The retention capacity of sample S20 is better than the retention capacity of sample S6 and its value is 1.0071 times higher than the value of S6. The retention capacity of

the carbonaceous clay sample taken in Gafsa (Tunisia)[17] is 1.5 times higher than that of S20 and S6. The retention capacity of the natural clay Marls from Gorna Oriahovitza (Bulgaria)[25] is 1.7 times higher than our two samples. Finally, the retention capacity of thermally activated clay Marls [25] is respectively 6.5 times higher than S20 and 6.6 times higher than S6.

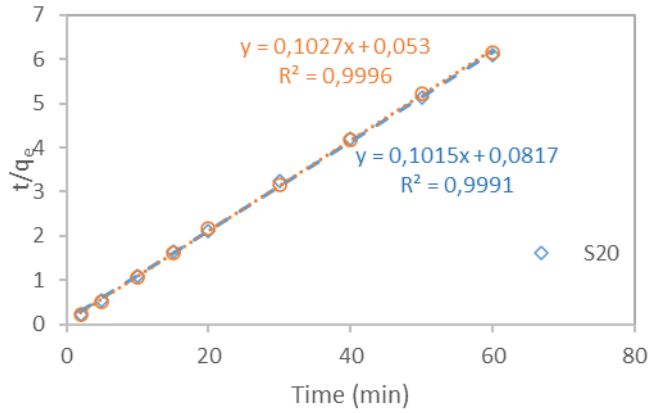

Fig 6. Pseudo-second-order equation of the retention of Zinc in Marl

Table 3 Retention capacity for different adsorbants ((*)- Gafsa, Tunisia, (**)- Gorna Oriahovitza, Bulgaria)

Materials	$pH_{initial}$	Concentration of Zinc (**mg/l**)	q_e (mg/g)	Auteurs
S20	5.5	20	9.94	This study
S6	5.5	20	9.87	This study
Carbonaceous clay (*)	6.0	19,61	15,21	A Sdiri. T. et al. (2014) [17]
Thermally activated clay Marl (**)	5,9	32,69	64,85	Stefanova R. Y. (2001) [25]
Natural clay Marls (**)	5,9	32,69	17,19	Stefanova R. Y. (2001) [25]

When the adsorption of zinc on the adsorbent only follows the intraparticle diffusion model, the straight line, which corresponds to the experimental data, must pass through the origin. In addition, when zinc adsorption is only controlled by liquid film diffusion, the fit data line must pass through the origin [26]. But in reality, the experimental data gives a straight line that does not pass through the origin and has an intercept. The intercept value characterizes the thickness of the boundary layer [27].

The liquid film diffusion model for the retention processes of S20 and S6 is illustrated in Figure 7. It is represented by two straight lines, which do not pass through the origin. The value of the rate constant for S20 is ki = 0.1479 mg/g.min and for S6 the value is ki = 0.0862 mg/g.min. This result indicates that the rate of the adsorption process for the case of S20 is 1.7158 times higher than that of S6. For S20, the thickness of the boundary layer is equal to Ci=8.6324, and for S6 Ci=9.0321 these low values indicate that the resistance to mass transfer is low [28].

For the intraparticle diffusion model, the retention process for S20 and S6 is represented by two straight lines with intercept (Fig. 8).The values of the rate constants in the case of S20 and S6 are kfd=0.0481mg/g.min and kfd=0.0233mg/g.min, respectively, these values indicate that the velocity of these processes is very low. The rate constant for S20 is 2.0643 times higher than the rate constant for S6. The resistance to mass transfer is very low, as indicated by the intercept values for S20 (Cfd=1.9939) and for S6 (Cfd=2.6135) [28]. The mass transfer resistance for S6 is 1.3107 times higher than the mass transfer resistance for S20.

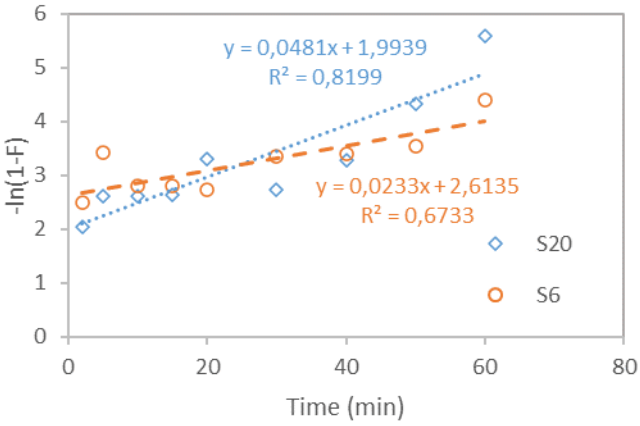

Fig 7. Liquid film diffusion for the Zinc adsorption in Marl

The values of the coefficients of determination (Table 5) for sample S20 indicate that the liquid film diffusion and intraparticle diffusion models simultaneously control the adsorption process and the same conclusion can be drawn for sample S6 [16].

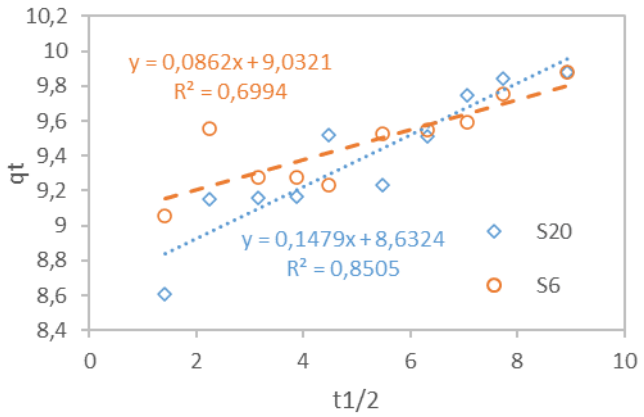

Fig 8. Intraparticle diffusion for the Zinc adsorption in Marl

Table 4: Liquid film diffusion and intraparticle diffusion parameters of Zinc adsorption

	Liquid film diffusion			Intraparticle diffusion		
	R^2	K_{fd} (mg/g.min)	C_{fd}	R^2	K_{id} (mg/g.min)	C_i
S20	0.8199	0.0481	1.9939	0.8505	0.1479	8.6324
S6	0.6733	0.0233	2.6135	0.6994	0.0862	9.0321

3.2.3. Two and three parameters isotherms study

In our work and for the study of two-parameter isotherms, four models are studied to describe the experimental results. The isotherm models studied are Langmuir, Freundlich, Temkin and Dubinin-Radushkevich. Langmuir developed his model with the following conditions: a single adsorption layer, adsorptions of one species per site, all sites are homogeneous, the adsorption is reversible and the adsorbed molecules do not interact with each other. The Langmuir equation is given by equation (15) [29][30]:

$$q_e = q_m \frac{K_L C_e}{1 + K_L C_e} \quad (15)$$

Where

q_e: the amount adsorbed at equilibrium (mg/g).

q_m: the maximum adsorption capacity (mg/g).

C_e: the equilibrium concentration (mg/L).

K_L : Langmuir constant (mg/L).

Freundlich equation is given by equation(16) [30]:

$$q_e = K_f C_e^{1/n_f} \quad (16)$$

K_f: is the parameter of the maximum capacity its associated with affinity of interaction energy.

n_f: characterize the system heterogeneity

The parameter of the maximum capacity K_f is associated with affinity of interaction energy. The value of $1/n_f$ is less than 1 and n_f characterize the system heterogeneity [15][29]. High values of K_f and n_f indicate a strong adsorption.

The Temkin isotherm equation (17):

$$q_e = \frac{RT}{b} \ln\left(A_T C_e\right) \text{[15][29]} \quad (17)$$

b: Temkin isotherm constant.

A_T: Temkin equilibrium binding constant.

q_e: the adsorbed amount at equilibrium (mg/g).

C_e: equilibrium concentration (mg/g).

T: the temperature in (°K).

R: the perfect gas constant. ($R=8.314\times10^{-3}$kJ.mole^{-1}.K^{-1}).

Dubinin-Radushkevich is given by equation (18):

$$\ln q_e = \ln q_m - \beta\varepsilon^2 \text{[15][29]} \quad (18)$$

ε is Polany potential defined by equation (19):

$$\varepsilon = RT \ln\left(1 + \frac{1}{C_e}\right) \quad (19)$$

β: activity coefficient (mole^2/J^2).

q_e: the adsorbed amount at equilibrium (mg/g).

q_m: the maximum adsorption capacity (mg/g).

C_e: equilibrium concentration (mg/L).

T: the temperature in (°K).

R: the perfect gas constant. ($R=8.314\times10^{-3}$kJ.mole^{-1}.K^{-1}).

The energy exchanged by one adsorbed mole is related by equation (20)

$$E = \frac{1}{\sqrt{2\beta}} \quad (20)$$

if E<8 kJ/mole there is predominance of physisorption, when8 kJ/mole<E<16kJ/mole ionique exchange is more viewed and if E>16kJ/mole there is a particular diffusion.

For the three parametres models, the Sips isotherm also nominate Langmuir-Freundlich isotherm, it is an association between Langmuir and Freundlich isotherms and its equation (21) [31, 32]is:

$$q_e = \frac{K_S C_e^{\beta_S}}{1 + a_S C_e^{\beta_S}} \quad (21)$$

K_s: the Sips isotherm model constants (L/g).

a_s: the Sips isotherm model constants (L/mg).

β_S: the Sips isotherm model exponent.

The Toth isotherm is an empirical model that improves the fitting of the experimental data of the Langmuir Model and gives a description of adsorption behavior in heterogeneous system. The Toth equation (22) [32]:

$$q_e = \frac{K_T C_e}{\left(a_T + C_e\right)^{1/t}} \quad (22)$$

K_T: the Toth isotherm constants (mg/g).
a_T: the Toth isotherm constants (L/mg).
t: the Toth isotherm constant.

The Redlish-Peterson isotherm is an empirical model, it's equation is (23) [32]

$$q_e = \frac{K_R C_e}{1 + a_R C_e^g} \quad (23)$$

K_R: the Redlish-Peterson isotherm constants (L/g).
a_R: the Redlish-Peterson isotherm constants(L/mg).
g: the Redlish-Peterson isotherm exponent.

Table 5: Parameters of Zinc adsorption isotherms

Langmuir			Freundlich			Temkin			Dubinin-Radushkevich		
	S20	S6		S20	S6		S20	S6		S20	S6
q_m (mg/g)	29,42	31,43	n_f	2,16	2,10	b	376,94	496,95	q_m (mg/g)	22,36	22,59
K_L (L/mg)	0,26	0,20	$1/n_f$	0,46	0,48	A_T(L/g)	2,56	5,67	β ($J^2/mole^2$)	9,6 10^{-7}	1,0 10^{-6}
R_L	0,16	0,20	K_f $(mg/g)(dm^3/g)^n$	7,24	6,98	---	---	---	E (kJ/mole)	0,721	0,693
R^2	0,96	0,94	R^2	0,95	0,98	R^2	0,96	0,89	R^2	0,88	0,83
R^2_{adj}	0,96	0,93	R^2_{adj}	0,93	0,98	R^2_{adj}	0,96	0,86	R^2_{adj}	0,84	0,79
AIC	23,39	26,33	AIC	25,92	19,41	AIC	23,48	30,15	AIC	30,89	32,74
AICc	27,39	30,33	AICc	29,92	23,41	AICc	27,48	34,15	AICc	34,89	36,74
χ^2	0,68	2,15	χ^2	1,41	0,41	χ^2	0,81	2,68	χ^2	4,77	5,91

For the Langmuir, Freundlich, Temkin and Dubinin-Radushkevich models, the nonlinear processing of the data is represented in the curves of figure 9 and 10 and the numerical results are grouped together in table 5. For the case of S20, the coefficient of determination and its fitted form indicate that Langmuir and Temkin are the best models. Followed, with a very small difference, by the Freundlich model and finally the Dubinin-Radushkevich model. This classification is clearer when using the parameters AIC, AICc and χ2. For S6 (fig. 10), the most representative model of our results (table 6) is the Freundlich isotherm referring to R2, R2adj, AIC, AICc and χ2 followed by Langmuir in second order, in the third order we have the Temkin model and finally it is the Dubinin-Radushkevich model.

The separation factor values for S20 are 1.25 times higher than the value for S6 and indicate that the Langmuir model is favorable. The value of the energy E exchanged by one adsorbed mole obtained from the Dubinin-Radushkevich model is less than 8 kJ/mole, so there is a predominance of physisorption in our adsorption process for both samples. The energy E exchanged by one mole adsorbed for S20 is 1.04 times higher than the corresponding value for the S6 case.

For the Toth, Sips and Radlish-Peterson isotherms, which are three-parameter models, the curves are shown in Fig. 11. and Fig. 12. Table 6 gives the results of the treatment.

For sample S20, the R-P model is the best model according to the coefficient of determination and its fitted form. In second position, we have Sips and Toth, with a very small difference for the values of the coefficients of determination and their fitted form. For S6, according to the values of the coefficient of determination and its fitted form, the best model is given simultaneously by Sips and Radlish-

Peterson, followed by the Toth model. The same classification of isotherms is obtained using the values of the nonlinear Chi-Square χ^2 test. The use of the parameters AIC and AICc allowed to make a choice between the Sips and Radlish-Peterson models, while the classical coefficients such as the coefficient of determination, its fitted form and the nonlinear chi-square test did not allow to make a split for the choice between the last two models.

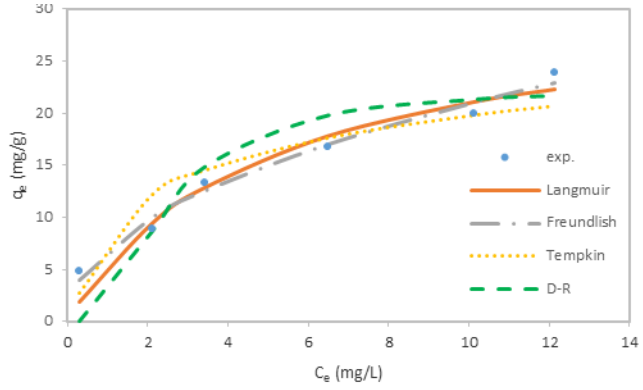

Fig 9. Two parameters isotherms of adsorption of Zinc in S20 marl sample (exp.: experimental)

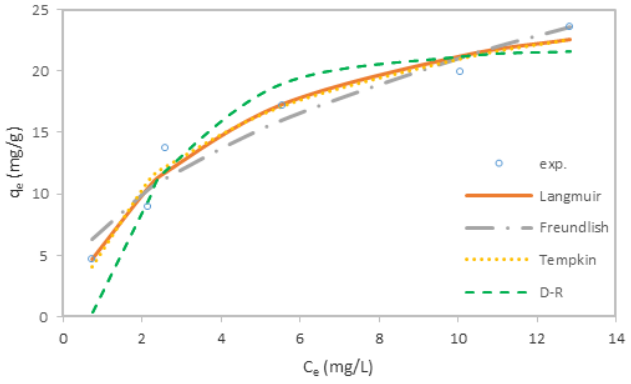

Fig 10. Two parameters' isotherms of adsorption of Zinc in S6 marl sample (exp.: experimental)

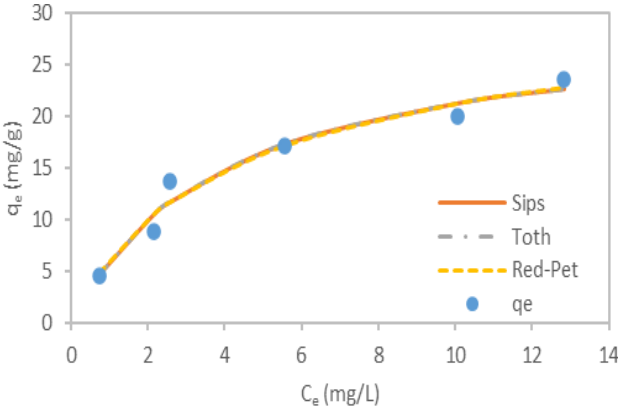

Fig 11. Three parameters' isotherms of Zinc adsorption in S20 marl sample

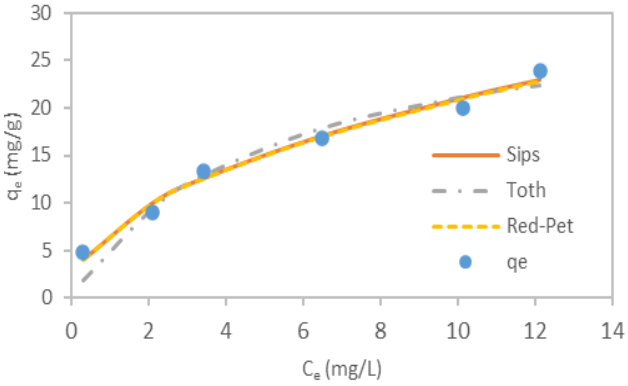

Fig 12. Three parameters' isotherms of Zinc adsorption in S6 marl sample

This result shows the importance that should be given to the use of the AIC and AICC parameters.

Table 6: Parameters of Zinc adsorption isotherms

Toth			Sips			Radlish-Peterson		
	S20	S6		S20	S6		S20	S6
K_T	29,42	31,43	K_S	7,61	6,98	K_R	8,30	10253,80
a_T	3,88	4,96	β_S	0,99	0,48	a_R	0,34	1455,46
t	1,00	1,00	a_S	0,26	0,00	g	0,93	0,53
R^2	0,96	0,94	R^2	0,96	0,98	R^2	0,97	0,98
R^2_{adj}	0,94	0,90	R^2_{adj}	0,94	0,97	R^2_{adj}	0,94	0,97
AIC	25,39	28,33	AIC	25,39	21,41	AIC	25,32	21,43
AICc	37,39	40,33	AICc	37,39	33,41	AICc	37,32	33,43
χ^2	0,68	2,15	χ^2	0,68	0,41	χ^2	0,69	0,41

4. Conclusion

The two samples of marl are collected in the same geological facies but at different depth. X-Fluorescence show the predominance of three compounds: silica, alumina and lime for the two samples. In FTIR analysis, all bands are identified for S20 and S6 and especially the bands characterizing the calcite. The specific surface area for S20 and S6 are equal respectively to 21.6206 m^2/g and 24.6445 m^2/g. The average pore diameter is equal to 78.5623 Å for S20 and 69.4124 Å for S6, so our materials have a meso-porous character.

The optimized parameters retained for adsorption are: pH=5.5 ± 0.2, masse of marl is 0.08g and contact time is 60 min.

For S20 the liquid film diffusion and intraparticle diffusion models control simultaneously the process of adsorption and the same conclusion can be done for the S6 sample.

The results of characterization obtained for the two samples S20 and S6, present a very great similarity. The values obtained by X-Fluorescence for S20 and S6 are very close and the small deviation is practically due to the errors related to the sample taking. All the bands of transmittance are identified for the two samples and their value have a small deviation. The BET characterization shows that the two samples have the same values with a small deviation for specific surface area, micro pores volume and average pore diameter.

For the isotherms with two and three parameters study, the two samples S20 and S6 have practically the same response to the models of isotherm studied her. The values of all parameters of isotherms present a great similitude.

Using AIC and AICc parameters gives a good opportunity to separate between results, when the coefficient of determination, its adjusted form and the non-linear chi-square test can't make a choice.

Conflict of Interest: The authors declare that they have no conflict of interest.

References

1. Musarrat J, Zaidi A, Saghir Khan M, Siddiqu MA, Al-Khedhairy AA. Contaminated soils in Almas Z , Khan M S, Goal R, Musarrat *J Biomanagement of metal*.2011; 323-342. http://dx.doi.org/10.1007./978-94-007-9_21
2. Lichtfous E, Schwarzbauer J, Robert D. Environmental Chemistry for a Sustainable World: *Remediation of Air and Water Pollution*. 2012; 379. http://dx.doi.org/10.1007./978-94-007-2442-6
3. Menacer S, Lounis A, Guedioura B, Bayou N. Uranium removal from aqueous solutions by adsorption on Aleppo pine sawdust, modified by NaOH and neutron irradiation. *Desalination and Water Treatment*. 2016; 57:34, 16184-16195. http://dx.doi.org/10.1080/19443994.2015.1077475.
4. Mukherjee S. Analytical Techniques for Clay Studies in: Mukherjee S. (eds) The science of clays Applications in Industry, Engineering and Environment. *Capital Publishing Company*.2013; 69-110. http://dx.doi.org/10.1007/978-94-007-6683-9_6
5. Farrah H, Hatton D, Pickering WF. The affinity of metal ions for clay surfaces. *Chem. Geolo*. 1980; 28: 55-68.
6. Zamzow M J, Murphy JE. Removing of metal cations from water using zeolites. *Sep. Sci. Technol*. 1992; 27: 1969-1984.
7. Zaidi S. Zeolites as Inorganic Ion Exchangers for Environmental Applications: An Overview in: Inamuddin and M. Luqman (eds), *Ion Exchange Technology II: Applications*, Springer, UK, 2012; 183-215. http://dx.doi.org/10.1007/978-94-007-4026-6.
8. Zinicovscaia I. Water quality A Major global problem in: Inga Zinicovscaia, L. cepoi (eds.) *Ceanobacteria for Bioremediation of Wastewaters*, Springer International Publishing Swetzerland; 2016,5-16. http://dx.doi.org/10.100/978-3-319-26751-7_2
9. Meetiyagoda TA, Fadilah K, Hagimori M, Senavirathna MD, Fujino T. Visualization and Quantification of the Impact of Humic Acid on Zinc Accumulation in Aquatic Plants Using a Low-Molecular-Weight Fluorescent Probe. *Journal of Water and Environment Technology*. 2021;19(2):49-63.
10. Jelle Mertens, Erik Smolders Zinc in B. J. Alloway (ed.) Heavy metals in: *soils : trace metals and metalloids in soils and their bioavailability*. Springer Science+Business Media Dordrecht. 2013. 465-493.
11. Zaid U H, Shafaqat A, Muhammad R, Afzal H, Zaheer A, Nasir R, Faraht A. Role of Zinc in Alleviating Heavy Metal Stress in: M. Naeem et al. (eds.), *Essential Plant Nutrients*. Springer International Publishing AG. 2017. 351-366. http://dx.doi.org/10.1007/978-3-319-58841-4_14
12. Angus M, Brown A. step-by-step guide to non-linear regression analysis of experimental data using a Microsoft Excel spreadsheet. *Computer Methods and Programs in Biomedicine*. 2001; 65: 191–200.
13. Jose LB, Joseph J, Pignatello MT. ISOT-Calc: Aversatile tool for parameter estimation in sorption isotherms. *Computer and Geosciences*. 2016; 94: 11-17. http://dx.doi.org/10.1016/j.cageo.2016.04.008
14. Comuzzi C, Polese P, Melchior A, Portanova R, Tolazzi M. SOLVERSTAT: a new utility for multipurpose analysis. An application to the investigation of dioxygenated Co (II) complex formation in dimethylsulfoxide solution. *Talanta*. 2003;59(1):67-80.
15. Sandy MV, Kurniawan A, Ayucitra A, Sunarso J, Suryadi I. Removal of copper ion from aqueous solution by adsorption using LABORATORIES-modified bentonite (organo-bentonite). *Front. Chem. Sci. Eng*. 2012; 6(1): 58-66.

http://dx.doi.org/10.1007:s11705-011-1160-6
16. Wu XL, Zhao D, Yang ST. Impact of solution chemistry conditions on the sorption behavior of Cu(II) on Lin'an montmorillonite. *Desalination*. 2011; 269: 84-91. http://dx.doi.org/10.1016/j.desl.2010.10.046
17. Sdiri AT, Higashi T, Jamoussi F. Adsorption of copper and zinc onto natural clay single and binary systems. *Int J. Environ. Sci. Technol*. 2014 ; 11: 1081-1092. http://dx.doi.org/10.1007/s13762-013-0305-1
18. Remenárová L, Pipíška M, Horník M, Rozložník M, Augustín J, Lesný J. Biosorption of cadmium and zinc by activated sludge from single and binary solutions: Mechanism, equilibrium and experimental design study. *Journal of the Taiwan Institute of Chemical Engineers*. 2012;43(3):433-443. http://dx.doi.org/10.1016/j.jtice.2011.12.004.
19. Hamidi A, Mohd N, Kamar S. Heavy metals (Cd, Pb, Zn, Ni, Cu and Cr(III)) removal from water in malayzia post treatment by heigt quality limestone. *Bioresources technology*. 2008; 99: 1578-1583.
20. Unuabonah EI, Omorogie MO, Oladoja NA. Modeling in adsorption: Fundamentals and Applications in Composite Nanoadsorbents. In G. Z. Kyzas A. C. Mitropoulos (eds) : *composite nanoadsorbents*, Elsevier; 2019; 85-118. http://dx.doi.org/10.1016/B978-0-12-814132-8.00005-8
21. Hamdaoui O. Batch study of liquid-phase adsorption of methylene blue using cedar sawdust and crushed brick. *Journal of Hazardous Materials*. 2006; 135: 264-373. http://dx.doi.org/10.1016/j.jhazmat.2005.11.062
22. Lagergren S. About the theory of so-called adsorption of soluble substances. *Kungliga Svenska Vetenskapsakademiens. Handlingar*. 1898; 24:1-39.
23. Lyubchik S, et al. The kinetic parameters evaluation for the adsorption process at liquid-solid interface in: Alexandra B. Ribeiro, Eduardo P. Mateus, Nazaré Couto (eds) *Electrokinetic across disciplanes and continents*. Springer. 2016; 81-109. http://dx.doi.org/10.1007/978-3-319-20179-5_5.
24. Ogata F, Iwata Y, Kawasaki N. Kinetics and Equilibrium Investigation of Cobalt(II), Nickel(II), and Tungsten(VI) Adsorption on Fly Ash Processed by Hydrothermal Treatment in an Alkaline Solution. *Journal of Water and Environment Technology*. 2015;13.
25. Stefanova RY. Metal removal by thermally activated clay marl. *J. Environ. Sci. Health Part A*. 2001; 36(3): 293-306. http://dx.doi.org/10.1081/ESE-100102923
26. Chen S, Shen W, Yu F. Huaping Wang Kinetic and thermodynamic studies of adsorption of Cu^{2+} and Pb^{2+} onto amidoximated bacterial cellulose. *Polym. Bull*. 2009; 63:283-297. http://dx.doi.org/10.1007/s00289-0009-0088-1
27. Lim SF, Yung A, Lee W. Kinetic study on removal of heavy metal ions from aqueous solution by using soil. *Environ. Dci. Pollut. Res*. 2015; 22:10144-10158. http://dx.doi.org/10.1007/s11356-015-4203-6
28. Mahtab A,et al. Modeling adsorption kinetics of trichloroethylene onto biochars derived from soybean stover and peanut shell wastes. *Environ. Sci. Pollut. Res*. 2013; 20:8364-8373. http://dx.doi.org/10.1007/s11356-013-1676-z
29. Jianzhong G, Shunwei C, Li L, Bing L, Ping Y, Lijun Z, Yanlong F. Adsorption og dye from waste water using chitosan-CTAB modified bentonites. *Journal of Colloid and Interface Science*. 2012; 382: 61-66. http://dx.doi.org/10.1016/j.jcis.2012.05.044
30. Nguyen VH, et al. Highly effective adsorption of organic dyes from aqueous solutions on longan seed-derived activated carbon. *Environmental Engineering Research*. 2023; 28(3):220116. https://doi.org/10.4491/eer.2022.116
31. Keng-Tung Wu, et al. A novel approach to characterizing liquid-phase adsorption on highly porous activated carbons using the Toth equation. Chemical Engineering Journal 2013; 221, 373-381. http://dx.doi.org/10.1016/j.cej.2013.02.012
32. Foo KY, Hameed BH.Insights into the modeling of adsorption isotherm systems. *Chemical Engineering Journal*. 2010; 156: 2-9. http://dx.doi.org/10.1016/j.cej.2009.09.013

Recommended Citation

Bellaloui M, Bennemla M, Semaoune F, Larbaoui D, Otsmane D, Melhania Y, Amranea A, Ladjouzia S. Contribution to characterization of the Zinc retention by marl collected from the aquifer substratum. *Alger. J. Eng. Technol. 2023*; 08(2):201-211. https:/dx.doi.org/10.57056/ajet.v8i2.124